JOURNAL OF APPLIED ELECTROCHEMISTRY 22 (1992) 230–234

Secondary aluminium–iron (III) chloride batteries with a low temperature molten salt electrolyte

F. M. DONAHUE*, S. E. MANCINI, L. SIMONSEN

Minotaur Technologies, Ann Arbor, MI 48103-4115, USA

Received 11 January 1991; revised 7 May 1991

Secondary aluminium–iron (III) chloride batteries using a low temperature molten salt electrolyte were constructed and tested. Discharge current densities were in the range 5 to 100 mA (~ 1 to 20 mA cm^{-2}; $\sim C/4$ to $5C$); charging currents were 5 mA ($C/4$ to $C/2$). Utilization of the positive electrode reactant was low due to the discharge rates and loading procedure. The mode for self discharge was dissolution of the positive electrode reactant and transport to the aluminium negative electrode where it reacted.

1. Introduction

Low temperature molten salts based on mixtures of organic salts (e.g. butylpyridinium chloride, 1-methyl-3-ethylimidazolium chloride (MEIC), and 1,2-dimethyl-3-propylimidazolium chloride (DMPIC)) and aluminium chloride have been proposed as battery electrolytes [1–6]. Binary solutions of these types are normally called basic (organic salt-rich), neutral (equimolar), and acidic ($AlCl_3$-rich).

Many of the physical properties (density, conductivity, and viscosity) of some of these (and similar) electrolytes have been measured and correlated with melt composition [7–9]. Conductivities of these ambient temperature molten salts compare very favourably with non-aqueous systems, but the viscosities are significantly higher. The shear rate dependence of the viscosity of MEIC-$AlCl_3$ melts has been investigated and found to be almost negligible [10]. Although the physical properties of these electrolytes have been well-studied, very little effort has been expended in investigating these melts in battery configurations which might lead to high energy density batteries.

Some battery systems which might use these low temperature molten salts (or ternaries based on them) are shown in Table 1. The standard cell voltages (computed from 'standard free energy of formation' data for the chemical species in the chemical reactions, *as written*) and the theoretical gravimetric energy densities, TGED, (computed from the standard cell voltages, specific capacities, and stoichiometries of the processes) are large and comparable to aqueous and nonaqueous systems currently in use. With the exception of the magnesium battery system (magnesium would displace aluminium from acidic melts), those listed are theoretically capable of being recharged, i.e. can be used in secondary battery configurations.

Some research on single cells using low temperature molten salts has been reported. These include Al/$FeCl_3$ primaries in basic MEIC binary melts [1, 2]. Primary Al/WCl_6 and Al/Br_2 cells were studied in basic MEIC melts [2]. Secondary batteries with MEIC-containing electrolytes were studied which also incorporated the characteristics of concentration cells [2]. Al/Cl_2 primary and secondary configurations were tested in basic and acidic melts, respectively; solubility of chlorine in the electrolyte caused significant self-discharge at the negative electrode in both electrolytes and, in the case of the acidic melts, resulted in chlorination of the organic cation [4, 11]. An Al/Cl_2 acidic (using DMPIC as organic salt), secondary battery was studied with an intercalated positive (eliminating the chlorine solubility problem alluded to above) [5].

Primary and secondary configurations of Al/Cl_2, Al/$FeCl_3$, and Al/$CuCl_2$ cells and primary configurations of Mg/Cl_2, Zn/Cl_2, Zn/$CuCl_2$, and Zn/$FeCl_3$ were reported with reticulated vitreous carbon (RVC) and, in the cases of chlorine, graphite current collectors as the positive electrodes [6]. It was found that chlorine (see above) and the metal chlorides were soluble in the basic melts – leading to self-discharge. The electrolyte for the chlorine positive studies was prepared with the pre-chlorinated cation, i.e. 1-methyl-3-ethyl-4,5-dichloroimidazolium chloride (MEDCIC), instead of the MEIC in order to obviate the loss of capacity from the cation chlorination process. This change caused an increase in the viscosity and melting point, but did not substantially alter the solubility of chlorine in the melts and the subsequent self-discharge process. It had been suggested that the addition of benzene to a basic melt caused insolubility of $FeCl_3$ [1] and that addition of cosolvents (e.g. benzene, nitriles, etc.) led to decreased viscosity and increased conductivity [7]. While the latter was found to be true, the former was not. Likewise, the addition of benzene to acidic melts substantially increased the solubility of the iron chlorides.

Addition of nitriles and other organic bases to acidic binaries caused a quantitative reaction with $Al_2Cl_7^-$ yielding aluminium-containing cationic

* Permanent address: Department of Chemical Engineering, The University of Michigan, Ann Arbor, MI 48109-2136, USA.

0021-891X/92

Table 1. Potential low temperature molten salt batteries

Reaction	*Standard Cell Voltage/V*	*Theoretical gravimetric energy density/Wh kg^{-1}*
$Mg + Cl_2 = MgCl_2$	3.07	1748
$Al + \frac{3}{2}Cl_2 = AlCl_3$	2.18	1315
$Al + \frac{3}{2}Br_2 = AlBr_3$	1.69	925
$Zn + Cl_2 = ZnCl_2$	1.92	748
$Cd + Br_2 = CdBr_2$	1.54	432
$Al + 3\ CuCl_2 = AlCl_3 + 3\ CuCl$	1.75	327
$Al + 3\ FeCl_3 = AlCl_3 + 3\ FeCl_2$	1.85	290
$Zn + 2CuCl_2 = ZnCl_2 + 2\ CuCl$	1.49	239
$Zn + 2\ FeCl_3 = ZnCl_2 + 2\ FeCl_2$	1.60	220

species, which could not be electrochemically reduced to produce metallic aluminium [12]. Additions of benzonitrile and acetonitrile (and other bases) to acidic melts have been shown to enhance the electrochemical dissolution rates of aluminium and magnesium [13]. Therefore, low temperature molten salt-based ternaries with these reactive solvents could only be used in primary configurations with aluminium negatives.

This work reports on experiments with $Al/FeCl_3$ cells in secondary battery configurations at ambient temperature in an acidic binary electrolyte of MEIC and $AlCl_3$ ($AlCl_3$ mole fraction = 0.58).

2. Experimental details

2.1. *Cell construction*

The battery configuration was that used previously [6]. The positive electrode current collector was made from RVC. The negative electrode was a cylindrical piece of aluminium. Current was carried away from the cell at the positive by a platinum wire which had been soldered to a platinum foil which contacted the RVC. Current was carried away from the negative by a stainless steel rod which had been threaded to connect with the top of the aluminium cylinder (which was drilled and tapped).

2.2. *Positives: reactants/current collectors*

Reticulated vitreous carbon (RVC) was used as the current collector. The previous study used 20 pore per inch (p.p.i.) product [6]. Unpublished studies indicated that smaller pore sizes (i.e. larger p.p.i. values) increased the apparent utilization of positive reactant; it was proposed that better contact between the precipitated reactant and the porous matrix was the cause of this effect [12]. In addition, decreasing the thickness of the current collector also increased the apparent utilization of positive reactant; it was proposed that this was due to the shorter transport distance within the matrix [12]. The experiments reported here (except where comparison is made to other configurations) used 70 p.p.i. RVC which was 0.48 cm thick. Its projected area (normal to current flow) was 4.9 cm^2.

The positive reactant was introduced into the current collector by an evaporative impregnation process. The $FeCl_3$ was deposited from a benzene slurry/solution in sealed containers using heat combined with partial vacuum. The solid active material was more-or-less uniformly distributed throughout the RVC matrix.

2.3. *Negative electrodes*

The negative electrodes were commercially pure aluminium cylinders which were machined to a diameter of 2.2 cm (3.8 cm^2 surface area for the circular face) and drilled and tapped on one end (to accommodate the stainless steel current collector, see above). Aluminium was chosen for these studies since it had been demonstrated previously that aluminium was reversible and could be used in a secondary battery configuration [5, 6]. Zinc was not studied since recent work showed that this electrode was not reversible in basic electrolytes [12] and, since its estimated reversible potential was close to that of aluminium in acidic solutions (formation of alloys would be expected during charge), its reversibility was not established in the acidic melts.

2.4. *Electrolytes*

The electrolytes were binary MEIC–$AlCl_3$ mixtures ($AlCl_3$ mole fraction = 0.58). The MEIC was synthesized and recrystallized and the $AlCl_3$ was sublimed by modifications of the methods given by Wilkes *et al.* [14]. Electrolytes were prepared and single cell batteries were assembled in a VAC Dry Box (moisture < 1 p.p.m.; oxygen < 10 p.p.m.). The electrolyte volume was approximately 6 cm^3 and flooded the positive electrode as well as filling the space between the electrodes. The electrode spacing varied between 2 and 4 mm. Batteries were brought into the room environment for testing at ambient temperature ($\sim 25°$ C).

2.5. *Battery testing procedure*

The assembled single cell batteries were connected to a galvanostat/potentiostat (Amel Model 551 or PARC Model 363) set in the galvanostatic mode. The

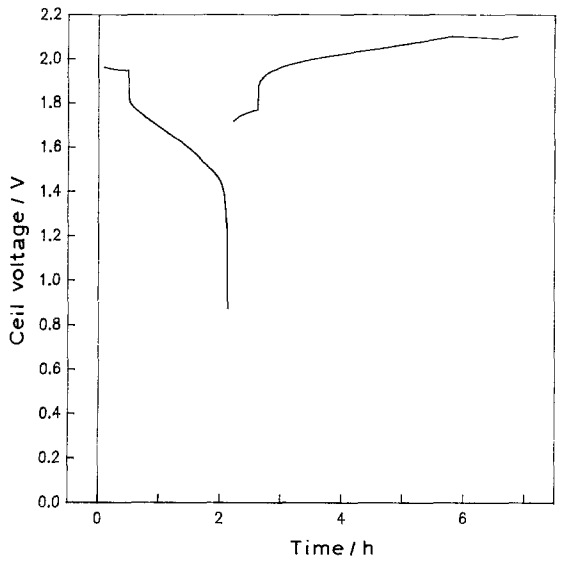

Fig. 1. Example of the discharge–charge battery testing procedure. The initial branch is 30 min on open circuit, discharge at 10 mA until a cutoff of 0.9 V, open circuit for 30 min, and charge at 5 mA until a cutoff of 2.1 V.

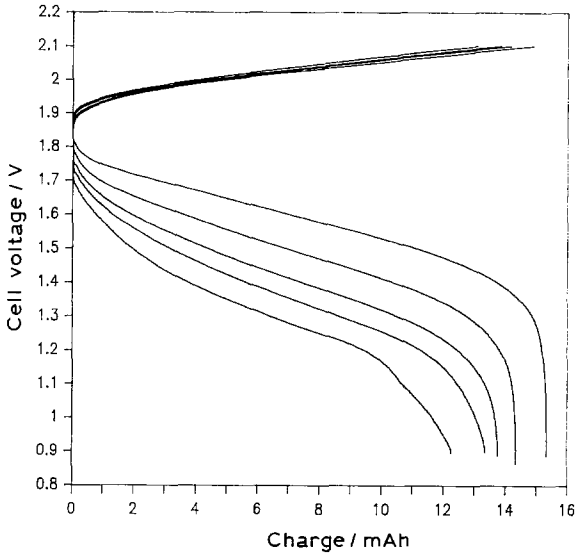

Fig. 2. Discharges at 15 to 35 mA (~ 3–7 mA cm^{-2}; 1–2.3 *C*) in 5 mA increments with a 90 mAh nominal capacity (based on loaded $FeCl_3$) battery. Charges were 5 mA.

potentiostat/galvanostat, in turn, was connected to a data acquisition (IBM Data Acquisition and Control Adapter [DACA] board) which was inserted in a full-length expansion slot of an IBM Computer (PC or PC/XT). The galvanostat was programmed to perform a series of 'open circuit – discharge – open circuit – charge' steps at fixed current(s) during the charge and discharge steps using a BASIC program developed at the University of Michigan [6]. The maximum (cut-off) charging voltage and minimum (cut-off) discharge voltage were assigned by the operator. Normally, the former was 2.2 V (low enough to avoid chlorine evolution) and the latter was 0.9 V. In most cases, the charging current was 5 mA. An example of voltage–time behaviour for an experimental battery is shown in Fig. 1 for and 'open circuit – 10 mA discharge – open circuit – 5 mA charge' sequence. The cell voltage was monitored using a Keithley Model 197/1972 Digital Multimeter with a strip chart Recorder.

3. Results and discussion

3.1. *Battery chemistry*

The overall reaction for the $Al/FeCl_3$ cell is

$$Al + AlCl_4^- + 3\ FeCl_3 = Al_2Cl_7^- + 3\ FeCl_2 \quad (1)$$

For these computations and most of the analyses presented here, the iron chloride species are assumed to be insoluble in this melt (while this is an unwarranted assumption [15], it does not significantly alter the conclusions presented here). The standard cell voltage is 1.85 V (see Table 1). A second discharge reaction is possible (standard cell voltage ~ 0.75 V) at deep discharges:

$$Al + \tfrac{3}{2}FeCl_2 + AlCl_4^- = Al_2Cl_7^- + \tfrac{3}{2}Fe \quad (2)$$

With a lower (discharge) voltage cutoff of 0.9 V, this second plateau was avoided in these studies.

Plots of cell voltage against charge passed (Fig. 2) show that sloping discharge curves were observed experimentally and that the slope increased with increasing discharge current. With ionic species as reactants and products (i.e. the chloroaluminate anions) in the overall reaction, one anticipates sloping voltage–time behaviour on discharge and charge provided that the concentration of one or both of the species changes during the charge or discharge. During discharge (left-to-right in Equation 2), the electrolyte becomes more acidic. In the systems studied here the mass of the electrolyte was approximately 8 g (6 cm^3), and the discharges were substantially less than 100 mAh; hence, it can be shown that the 'gross' composition of the electrolyte did not change substantially. Therefore, sloping discharge–charge data could not be ascribed to compositional changes in the bulk electrolyte.

The reaction at the positive electrode is

$$FeCl_2 + 2\ AlCl_4^- = FeCl_3 + Al_2Cl_7^- + e^- \quad (3)$$

During discharge (*i.e.* when this reaction proceeds from right to left), unlike the overall cell 'chemistry', the positive electrode (and its environs) becomes more basic. The computed changes in composition within the RVC current collectors for the systems studied were too low to be the cause of the sloping discharge curves.

3.2 *Effect of cycling on behaviour*

Figure 3 shows cell voltage–charge data for a single cell battery (106 mAh nominal capacity based on $FeCl_3$ loading; *C*-rate* ~ 19 mA) undergoing cycling. All of the discharges were at 10 mA while the charges were at 5 mA. The first discharge (curve a) is typical of

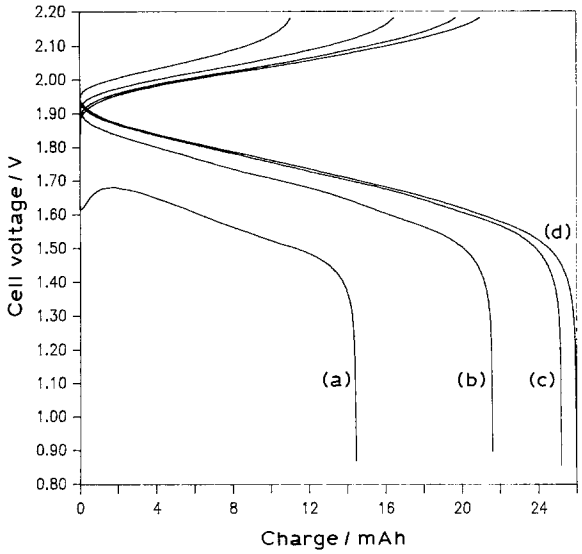

Fig. 3. Successive start-up discharges at 10 mA. Charges were at 5 mA.

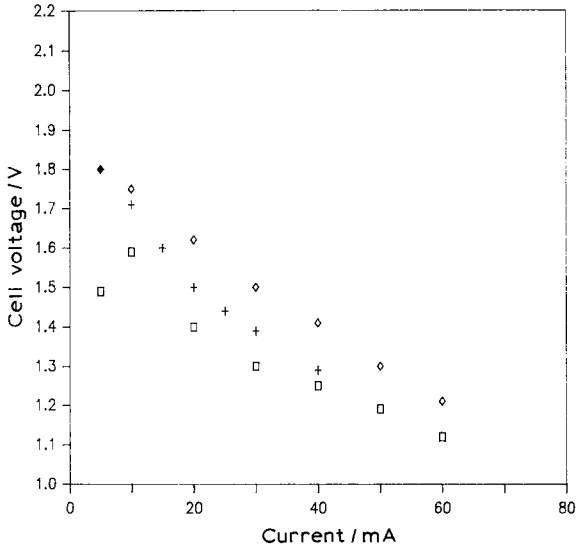

Fig. 4. Polarization behaviour of 57 mAh nominal capacity (based on loaded $FeCl_3$) battery. Key: initial data (□), second data set (+) third data set, (◇).

many other batteries in this study, i.e. the cell voltage experiences a minimum before assuming a typical sloping discharge. In addition, subsequent discharges (b–d) show progressively improved behaviour, e.g. increased capacity and increased (to a limit) cell voltage under load. A parallel effect is observed for the charging curves, i.e. the cell voltage during charging decreases with cycling. It can be noted that, for these experiments, the apparent capacity restored during charging was less than that removed on discharge. This is due to two effects (both experimental artifacts), *viz.* the assigned cut-off voltage on charge was too low (note that the voltage had not risen sharply at cut-off) and the battery was undergoing charging on 'open circuit' (the BASIC computer program fixes the 'zero current' condition based on a null point in the galvanostat/potentiostat; it was found that the null point for the PARC Model 363 tended to drift on 'start-up' – when the instrument was kept 'on' continuously the problem was overcome).

The progressive improvement of the cell properties at successive 10 mA discharges was also reflected in cells where the discharge sequence was set at different currents. Figure 4 shows the current–voltage behaviour for a battery (57 mAh nominal capacity; *C*-rate ~ 10 mA) on successive cycling. The cell voltages are the mean values computed from

$$E_{\text{mean}} = (1/t_{\text{co}}) \int E(t)\, \mathrm{d}t \qquad (4)$$

where t_{co} is the time (h) to cutoff and the integration is carried out over the discharge from initiation to cutoff. The data for the initial discharge set (squares) were consistently lower than subsequent discharge sets; in addition, successive improvement was observed for the second and third sets. Notice, also, that the initial discharge (5 mA) result was substantially lower than that observed for subsequent discharges (see also curve a in Fig. 3) and for discharges in the initial set at higher currents. This behaviour is characteristic of all batteries tested, i.e. cycling of the batteries led to improved (to a limit) cell behaviour. It is believed that this improvement resulted from rearrangement of the active material within the RVC matrix with cycling in some sort of dissolution-precipitation process. It is further believed that the improvement in the cell voltage behaviour is a function of the available matrix reaction sites on the positive current collector and not on the loading of the active material (see below).

3.3. *Utilization of active material at the positive*

Another characteristic of the batteries constructed and tested here was that the nominal capacity was always much greater than the capacity at cut-off or the estimated *C*-rate current. The latter is shown in Fig. 5 where data for five of the batteries is plotted. Since examination of scanning electron micrographs (SEM) of loaded positives showed that most of the deposits were not in intimate contact with the current collector

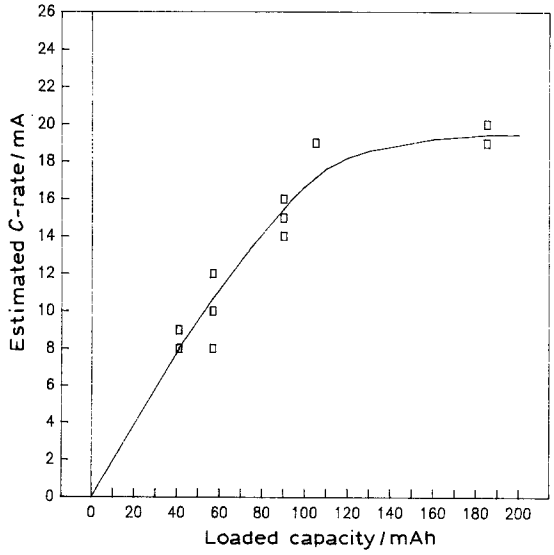

Fig. 5. Plot of estimated *C*-rate against loaded ($FeCl_3$) capacity.

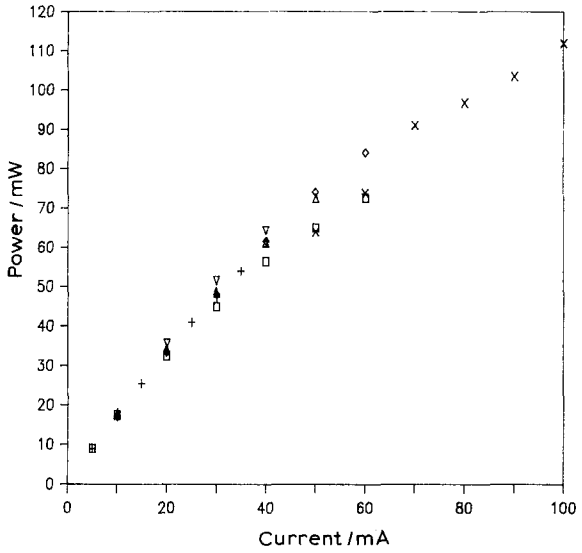

Fig. 6. Plot of battery power against cell current for six of the batteries. Loading capacity/mAh: (△) 41, (□) 57, (+) 90, (▽) 105, (×) 106 and (◇) 185.

[15], it is evident that such material is not available for electrochemical reaction.

In addition to the 'unavailability' of much of the loaded positive active material, the utilization of the active material is dependent on the discharge current (see Fig. 2). This type of behaviour is not unusual for flooded porous electrode batteries and is often the cause of sloping discharge curves. A model under development [15] has shown that some, but not all, of the sloping is due to non-uniform utilization of active material, at high current densities local loss of active material is predicted.

3.4. *Power–current behaviour*

Figure 6 shows the power–current behaviour for those batteries where the current was varied over a reasonable range. The power was computed from the product of the mean cell voltage (see above) and the discharge current. The data were for 'subsequent' (rather than 'initial') discharges. It is evident that, for currents less than 40 mA (discharge rates in excess of $2C$ for all batteries studied), there was virtually no dependence of active material loading on the discharge voltage at fixed current. In addition, at higher rates, the difference did not seem to depend on loading. One concludes that the current–voltage behaviour was independent of the battery loading, but, coupled with results from previous studies [6, 12], was dependent on the positive electrode matrix.

3.5. *Self-discharge/internal shorting*

Self-discharge is possible due to the solubility of $FeCl_3$ in the electrolyte. This capacity loss was not obvious in the electrochemical studies since there was a substantial excess quantity of both the positive active material and the aluminium negatives. However, on a number of occasions, dendritic deposits (most likely $FeCl_2$) were observed on the aluminium electrodes. On these occasions there was no obvious evidence of diminished battery performance.

On other occasions, apparent internal shorting occurred. Open circuit cell voltages were observed which were below the 0.9 V cut-off and, following charging to the upper cutoff voltage, were able to continue the discharge-charge regimen. In each case, no internal shorts were seen and external shorts were verified as absent; the cause of phenomenon is unknown at this time.

4. Conclusions

Secondary batteries were constructed and tested at discharge currents in the range of 5 to 100 mA (~ 1 to 20 mA cm^{-2}; $\sim C/2$ to $5C$). Sloping discharge curves were observed which could be partially ascribed to non-uniform reaction within the positive electrode matrix, but was not due to composition changes within the matrix or bulk electrolyte. The mode of self-discharge was identified as dissolution of the active material in the positive current collector and transport to the aluminium negative.

Acknowledgement

This work had been supported by the US Air Force/ Department of Defense SBIR program under Contract Number F33615-88-C-2869 with ASD/PMRSA, Wright-Patterson AFB.

References

[1] D. Floreani, D. Stech, J. Wilkes, J. Williams, B. Piersma, L. King and R. Vaughn, 'Proceedings 30th Power Sources Symposium'. Electrochemical Society, Inc., Pennington NJ (1982) pp. 84–6.
[2] G. F. Reynolds and C. J. Dymek, *J. Power Sources* **15** (1985) 109.
[3] C. J. Dymek, G. F. Reynolds and J. S. Wilkes, *ibid.* **17** (1987) 134.
[4] F. M. Donahue, FJSRL-TM-84-002. Frank J. Seiler Research Laboratory, USAF Academy, CO (1984).
[5] P. R. Gifford and J. B. Palmisano, *J. Electrochem. Soc.* **135** (1988) 650.
[6] L. R. Simonsen and F. M. Donahue, 'Proceedings 33rd International Power Sources Symposium'. Electrochemical Society, Inc., Pennington NJ, (1988) pp. 346–50.
[7] A. A. Fannin, L. A. King, J. A. Levisky and J. S. Wilkes, *J. Phys. Chem.* **88** (1984) 2609 and 2614.
[8] J. R. Sanders, E. H. Ward and C. L. Hussey, *J. Electrochem. Soc.* **133** (1986) 325.
[9] R. A. Carpio, L. A. King, R. E. Lindstrom, J. C. Nardi and C. L. Hussey, *ibid.* **126** (1979) 1644.
[10] J. F. Ross and F. M. Donahue, *J. Appl. Electrochem.* **19** (1989) 290.
[11] F. M. Donahue, J. A. Levisky, G. F. Reynolds and J. S. Wilkes, 'Proceedings of the 5th International Symposium on Molten Salts. Vol. 86-1. (Edited by M. Blander *et al.*) The Electrochemical Society, Pennington NJ (1986) pp. 332–7.
[12] F. M. Donahue and L. R. Simonsen, unpublished results.
[13] F. M. Donahue, L. R. Simonsen and R. Moy, U.S. Patent No. 4,882,244.
[14] J. S. Wilkes, J. A. Levisky, R. A. Wilson and C. L. Hussey, *Inorg. Chem.* **21** (1982) 1263.
[15] S. E. Mancini and F. M. Donahue, unpublished results.